Supplementary Information

A Urea-Integrated Molecular Phenothiazine Cathode via Hydrogen-Bonding Engineering for High-Performance Lithium Organic Batteries

*Jing Zeng, Shujuan Cao, Yanran Guo, Xiujuan Wang, Xiaoming He**

*To whom correspondence should be addressed

Key Laboratory of Applied Surface and Colloid Chemistry (Ministry of Education), School of Chemistry and Chemical Engineering, Shaanxi Normal University, Xi'an 710119, P.R. China

*Corresponding Author Email: xmhe@snnu.edu.cn

1. Materials

Ethyl isocyanate were purchased from Adamas. Poly(vinylidene fluoride) (PVDF), Ketjenblack(ECP-600JD) were obtained from Shenzhen Kejing Zhida Technology Co., Ltd. The lithium chip, CR2032 battery case and separator (Celgard2400) were purchased from DoDoChem. PVDF and Ketjen Black (ECP-600JD) were dried at 80 ºC for 12 h under vacuum oven before use. 3,7-diamino-N-methyl phenothiazine (MPT-NH_2) was prepared according to reported literature.[S1] All other reagents or solvents were used without further purification, unless indicated otherwise.

2. Instruments

^{1}H NMR and ^{13}C NMR spectra were obtained on 600 MHz BRUKER spectrometer. Mass spectrometry data were collected on a Bruker maxis UHR-TOF mass spectrometer. IR spectra were obtained on a PE-Frontier instrument. Thermogravimetric analysis (TGA) was performed under nitrogen atmosphere from 25 to 800 ℃ with a heating rate of 10 ℃ min^{-1}. EPR spectra were recorded on a Bruker E500 EPR spectrometer. The X-ray photoelectron spectra (XPS) experiments were carried out on a PHI-5400 electron spectrometer. Theoretical calculations were carried out at the B3LYP/6-31G(d, p) level by using the GAUSSIAN 09 suite of programs.[S2]

3. Synthesis of MPT-U

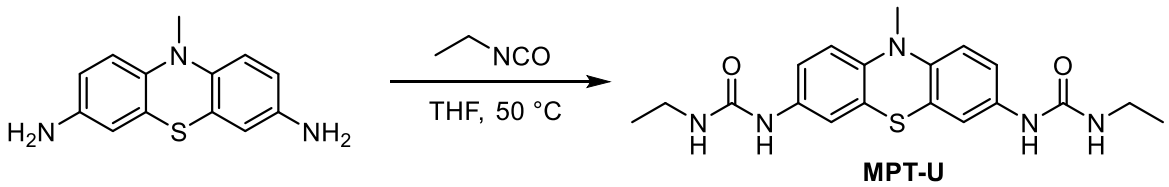

Scheme S1. Synthesis of MPT-U.

To a solution of 3,7-diamino-N-methyl phenothiazine (**MPT-NH_2**, 0.5 g, 2.06 mmol) in THF (25 mL), was added ethyl isocyanate (0.44 g, 6.20 mmol). The reaction mixture was stirred at 50 ºC for 24 h. During the reaction, large white precipitation formed. After cooling down to room temperature, the product was collected by filtration and washed with THF. Yield: 0.78 g, 98 %. ^{1}H NMR (600 MHz, DMSO-d_6): δ/ppm = 8.28 (s, 2H; NH), 7.32 (s, 2H; ArH), 7.11 (d, J = 8.4 Hz, 2H; ArH), 6.79 (d, J = 8.4 Hz, 2H; ArH), 6.02 (s, 2H; NH), 3.21 (s, 3H; NCH_3), 3.08 (t, J = 6.6 Hz, 4H; CH_2), 1.04 (t, J = 6.6 Hz, 6H; CH_3). ^{13}C NMR (150 MHz, DMSO-d_6): δ/ppm = 155.62, 140.05, 135.83, 122.44, 117.50, 116.86, 114.58, 35.30, 34.44, 15.94. HR-MS: m/z calculated for $C_{19}H_{24}N_5O_2S$ $[M+H]^+$ 386.1645, found 386.1649.

4. Battery Fabrication and Testing

The working electrodes were prepared by mixing the active material (MPT-U), conductive Ketjenblack (ECP-600JD), and PVDF binder in a weight ratio of 5:4:1 with NMP as a solvent. The resulting ink was cast onto the carbon-coating aluminum foil to prepare electrodes. The prepared electrodes were dried in a vacuum oven at 80 °C for 12 h to remove residual solvent. Then, the electrodes were cut into disks with a diameter of 12 mm and the mass loading of the active material was about 0.6-1.0 mg cm^{-2}. CR2032 coin-type coin cells were assembled in an argon-filled glove box. A lithium foil with a diameter of 16 mm was used as a counter electrode, a microporous polypropylene membrane (Celgard2400) was employed as a separator, and 3 M $LiClO_4$ in EC/DEC (1:1, v/v) was used as the electrolyte. The battery was left to stand for 12 hours before testing.

The battery performance data were measured on a LAND CT2001A battery system at 30°C with the voltage range of 2.5−4.4V. Cyclic voltammetry (CV) and electrochemical impedance spectroscopy

(EIS) tests of the batteries were performed on a CHI760E electrochemical workstation. Galvanostatic charge and discharge (GCD) and galvanostatic intermittent titration technique (GITT) tests were carried out using LANHE-CT2001A system (Wuhan, China) in the potential ranging from 2.5 to 4.4 V (vs. Li/Li^+) at different current densities.

5. Calculations of the Electrochemical Metrics

Theoretical capacity (C_{theor}, mAh g^{-1}) was calculated according to the equation (1):

$$C_{theor} = \frac{nF}{3.6 \times M} \quad (1)$$

where n is the number of electrons transferred per molecules, F is the Faraday's constant (96484 C mol^{-1}), M is molecular weight of the molecules.

The b-value and capacitive contribution at a particular potential were determined as follows:

The relationship between scan rate (υ, mV s^{-1}) in a CV and the corresponding cathodic or anodic peak current (i_p, A g^{-1}) is shown in equation (2).[S3] The b-value was the slope of the log(v)-log(i_p) plots according to equation (3).

$$i_p = av^b \quad (2)$$

$$\log(i_p) = \log(a) + b\log(v) \quad (3)$$

where a and b are adjustable parameters.

Moreover, the relationship between the current at a particular potential (i(V), A g^{-1}) and the scan rate (υ, mV s^{-1}) is shown in equation (4).[S4] Solving for the values of k_1 and k_2 at each potential, we can obtain the percentage of capacitive contribution the total current (k_2v/i(V)).

$$i(V) = k_1v^{1/2} + k_2v \quad (4)$$

6. Calculation of ion diffusion coefficients (D, cm^2 s^{-1}) from GITT

The value of ion diffusion coefficients could be calculated by the following equation: [S5]

$$D_{ClO4-} = \frac{4}{\pi\tau}\left(\frac{V_m m_B}{SM_m}\right)^2\left(\frac{\Delta E_s}{\Delta E_t}\right)^2$$

where τ is the duration of the current pulse (s), V_m is the molar volume of the active material (cm^3 mol^{-1}), m_B is the mass of the active material in the electrolyte (g), M_m is the molar mass of active material (g mol^{-1}), S is the contact surface area (cm^2) between electrode and electrolyte, ΔE_s is the equilibrium potential change induced by current pulse, ΔE_t is the potential variation during the constant current pulse.

7. Supplementary Schemes, Figures and Tables

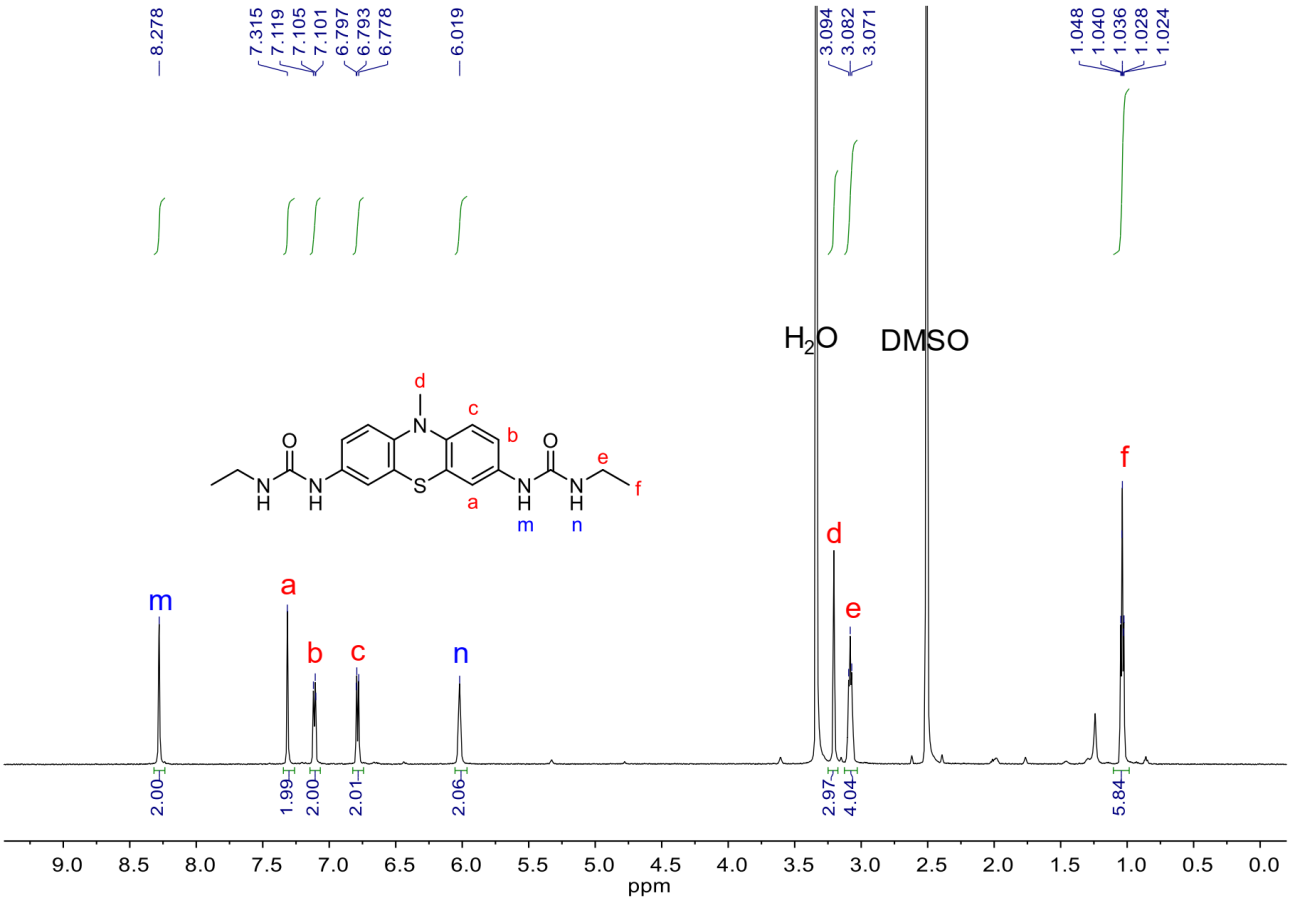

Figure S1. ^{1}H NMR spectrum of **MPT-U** in DMSO-d_6.

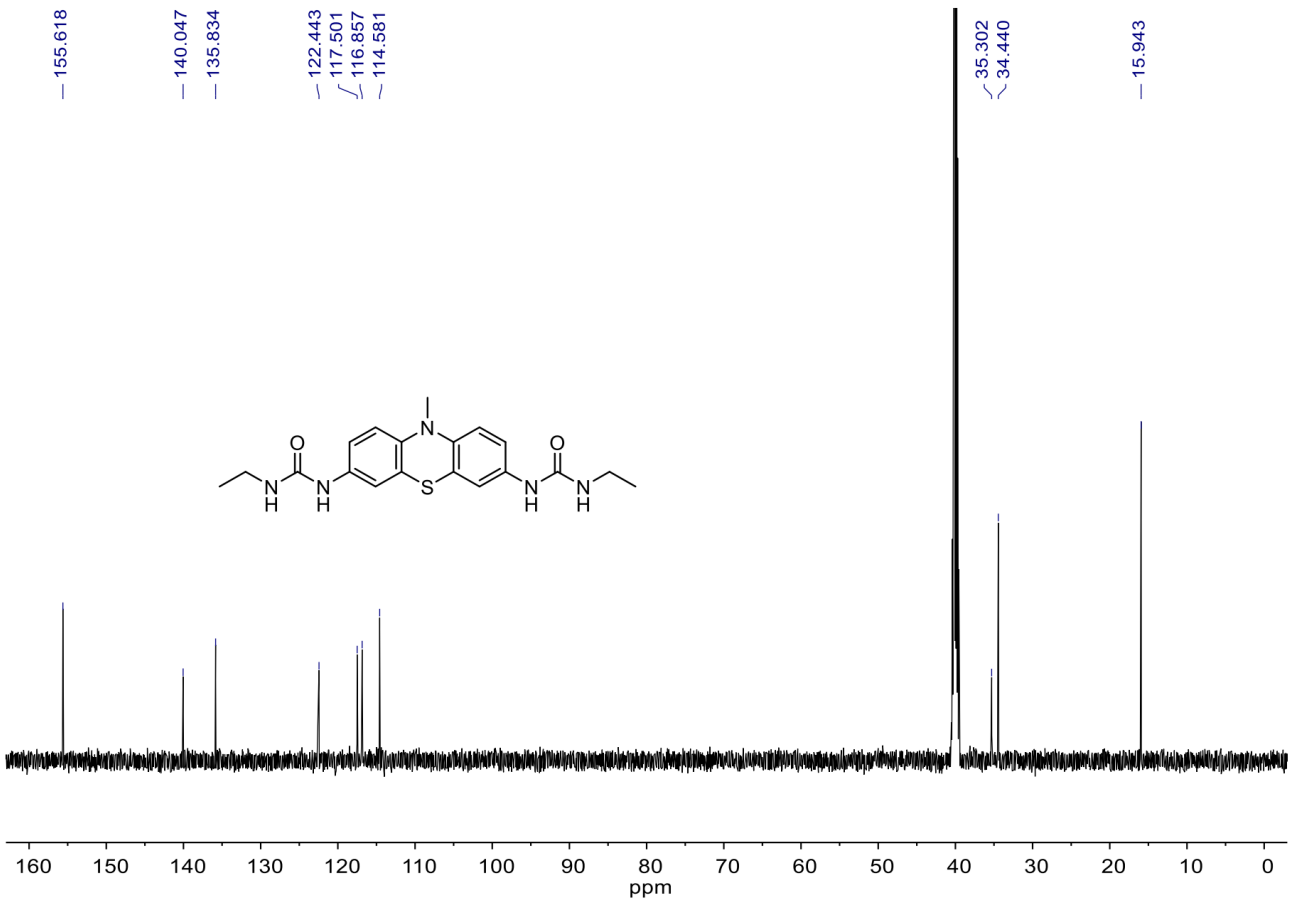

Figure S2. ^{13}C NMR spectrum of **MPT-U** in DMSO-d_6.

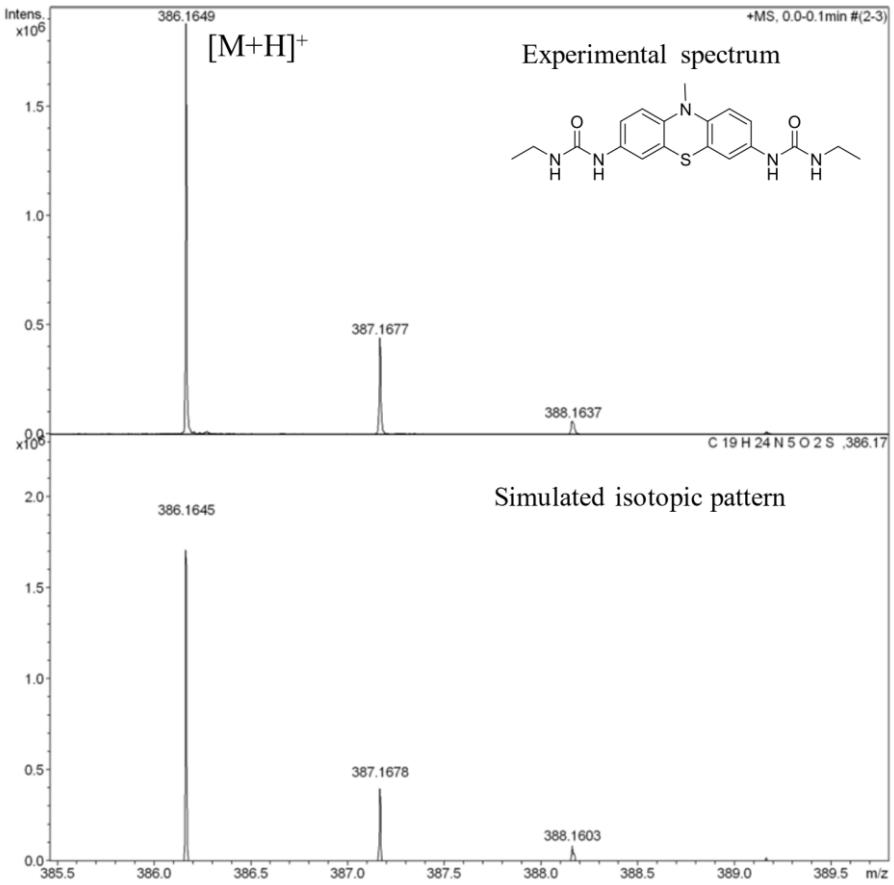

Figure S3. Mass spectrum of **MPT-U** in DMSO-d_6.

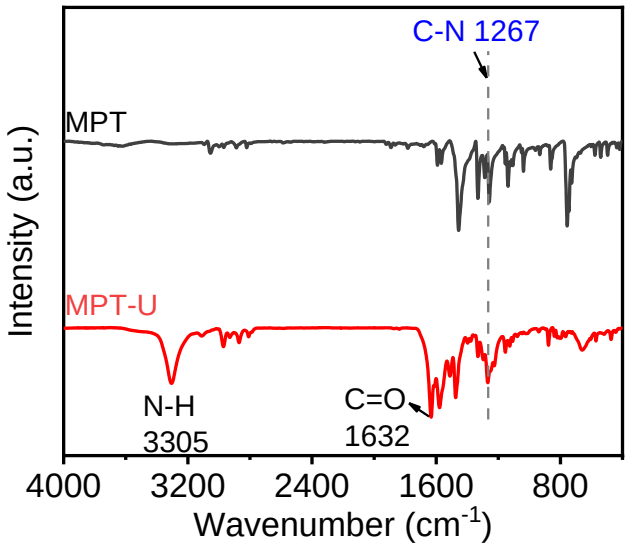

Figure S4. FT-IR spectra of MPT and MPT-U.

Solubility Test

Solubility of MPT: To 50 mg of MPT, EC/DEC (1:1, v/v) electrolyte was gradually added in 100 μL portions at 5-minute intervals until the MPT was fully dissolved.

Solubility of MPT-U: First, UV-vis spectra of MPT-U in DMSO at various concentrations were measured to construct a standard curve. Then, the UV-vis spectrum of MPT-U in a saturated EC/DEC (1:1, v/v) electrolyte was measured, and the solubility was calculated based on the standard curve (see Figure below).

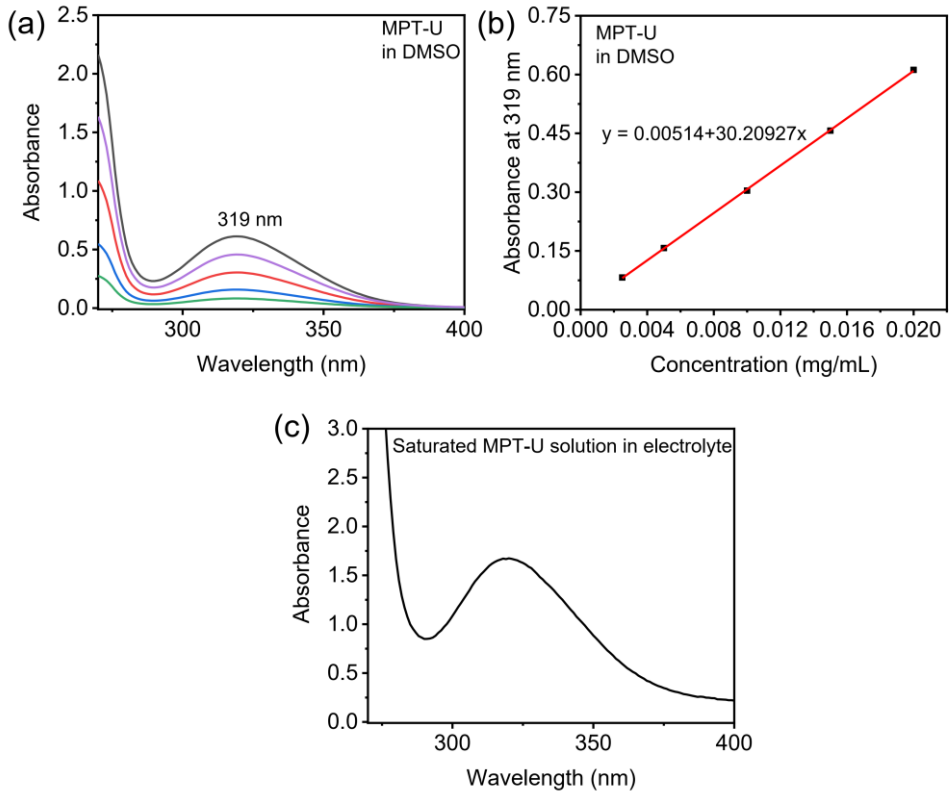

Figure S5. (a) UV-vis spectra of MPT-U in DMSO at different concentrations and (b) fitting curve of absorbance at 319 nm with concentration. (c) UV-vis spectrum of MPT-U in saturated EC/DEC (1:1, v/v) electrolyte solution.

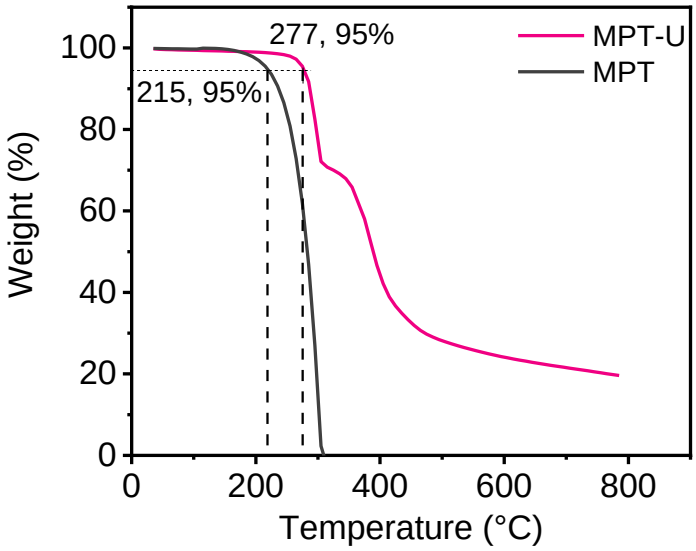

Figure S6. TGA curves of MPT and MPT-U.

Additional discussion: MPT begins to lose weight at ca. 170 °C and retains no weight when reaching 300 °C, indicating its high sublimability. In contrast, MPT-U exhibits high thermal stability, with their decomposition temperatures (T_d) of 277 °C.

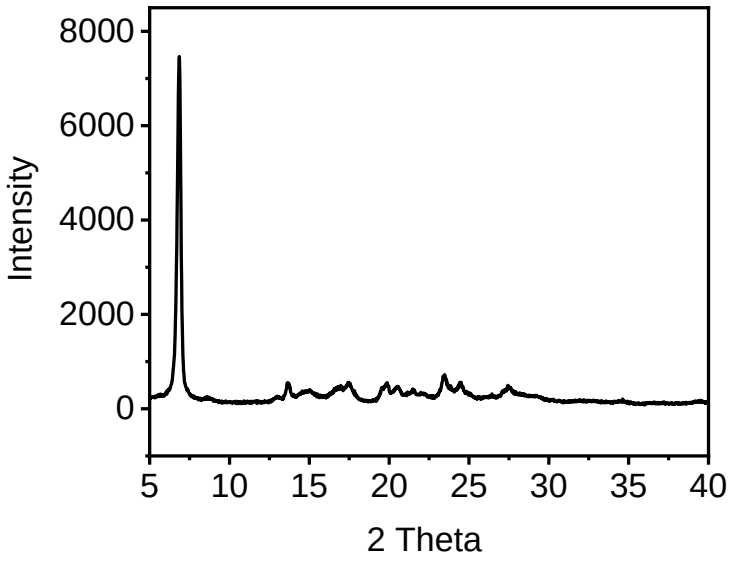

Figure S7. XRD spectrum of MPT-U.

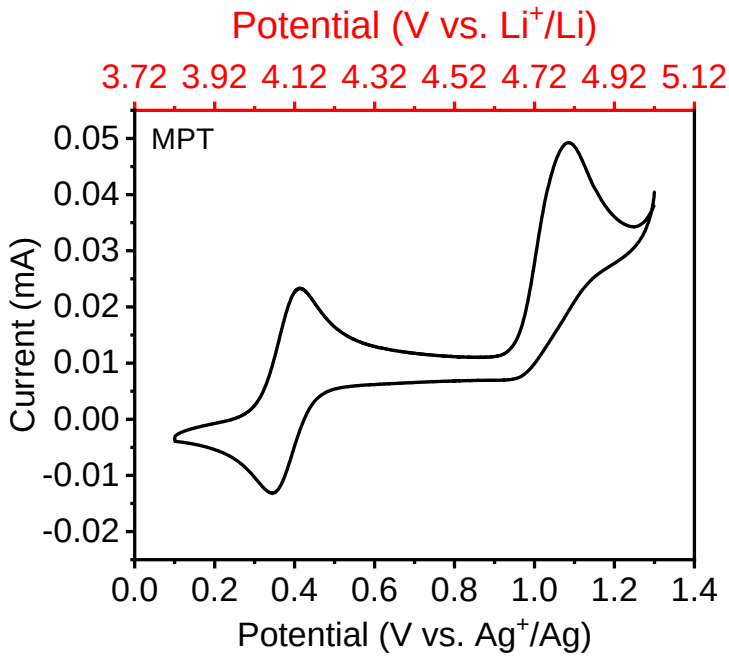

Figure S8. Cyclic voltammograms of MPT in CH_3CN solution (c = 1 mM) with 0.1 M *n*Bu_4NPF_6 as a supporting electrolyte at a scan rate of 100 mV s^{-1}. E (vs Li^+/Li) = E (vs Ag^+/Ag) + 3.72 V.

Table S1. Electrochemical comparison of current work and other reported phenothiazine-based organic cathodes in the literature for LOBs.

Materials (reference)	**Electrode Composition**	**C_{thero}** (mAh g^{-1})	**Specific capacity** (mAh g^{-1}) (**Current**)	**Cycle Stability** Retention /Cycles / Current	**Redox Window** (V)
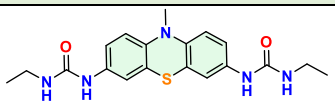 **MPT-U** **This work**	active material: ketjenblack: PVDF = 5:4:1	139	106 (0.2 A g^{-1}) 93 (0.5 A g^{-1}) 88 (1 A g^{-1}) 84 (2 A g^{-1}) 74 (5 A g^{-1}) 61 (10 A g^{-1})	73%/400/0.2 A g^{-1} 69%/2000/2 A g^{-1}	2.5-4.4 V
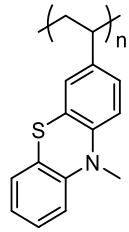 **PVMPT** *Energy Environ. Sci.*, **2017**, *10*, 2334-2341.	active material: Super P: PVDF = 5: 4.7: 0.3	112	56 (1 C) 50 (10 C) 26 (100 C) 1 C = 112 mAh g^{-1}	100%/1000/1 C 93.5%/10000/10 C	3-4 V
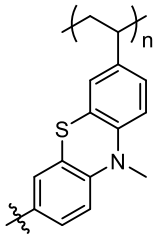 **X-PVMPT** *Adv. Energy Mater.* **2018**, *8*, 1802151.	active material: Super P: PVDF = 5: 4: 1	112	107 (1 C) 85 (10 C) 70 (20 C) 1 C = 112 mAh g^{-1}	95%/1000/1 C 95%/1000/10 C	3-4 V
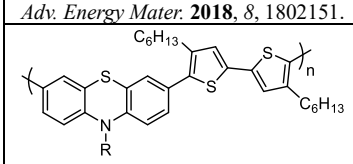 **P1a** *Adv. Funct. Mater.* **2019**, *29*, 1906436.	active material: Super P: PVDF = 6: 3.5: 0.5	36.4	34.7 (1 C) 32.7 (10 C) 1 C = 36 mAh g^{-1}	100%/100/1 C 100%/2200/10 C 97.5%/30000/100 C	3.2-3.9V
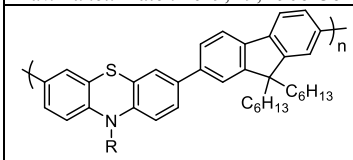 **P2** *Adv. Funct. Mater.* **2019**, *29*, 1906436.	active material: Super P: PVDF = 6: 3.5: 0.5	36.4	33.4 (1 C) 30.9 (10 C) 1 C = 36 mAh g^{-1}	98%/100/1 C 72%/2200/10 C	3.2-3.9V
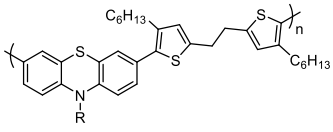 **P3** *Adv. Funct. Mater.* **2019**, *29*, 1906436.	active material: Super P: PVDF = 6: 3.5: 0.5	35.1	31.0 (1 C) 1 C = 35 mAh g^{-1}	100%/100/1 C	3.2-3.9V
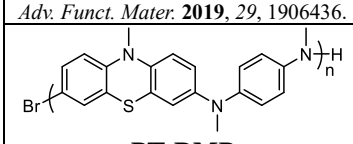 **PT-DMP** *ACS Appl. Energy Mater.* **2018**, *1*, 3560-3564.	active material: Super P: PVDF = 7: 2: 1	156	128 (1 C) 1 C = 156 mAh g^{-1}	64%/50/1 C	2.8-4.3V

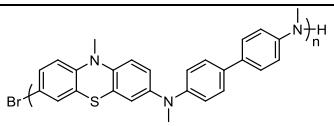 **PT-BZ** *ACS Appl. Energy Mater.* **2018**, *1*, 3560-3564.	active material: Super P: PVDF = 7: 2: 1	127	97 (1 C) 1 C = 156 mAh g^{-1}	66%/50/1 C	2.8-4.3V
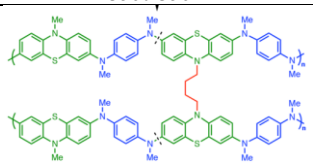 *ACS Appl. Energy Mater.* **2018**, *1*, 3560-3564.	active material: Super P: PVDF = 7: 2: 1	155	150 (5 C) 1 C = 155 mAh g^{-1}	74%/50/5 C	2.8-4.3V
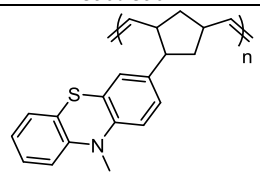 **PNMPT (**and **X-PNMPT)** *ChemSusChem* **2020**, *13*, 2232-2238.	active material: Super P: PVDF = 5: 4.5: 0.5	88	69 (1 C) 1 C = 88 mAh g^{-1}	97%/300/1 C 81%/1000/1 C	3.3-3.9V
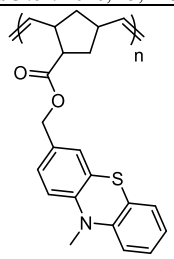 **P1** *ChemSusChem* **2020**, *13*, 2232-2238.	active material: Super P: PVDF = 5: 4.5: 0.5	74	62 (1 C) 1 C = 74 mAh g^{-1}	45%/300/1 C	3.3-3.9V
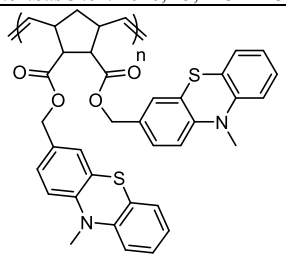 **P2** *ChemSusChem* **2020**, *13*, 2232-2238.	active material: Super P: PVDF = 5: 4.5: 0.5	86	73 (1 C) 1 C = 86 mAh g^{-1}	45%/300/1 C	3.3-3.9V
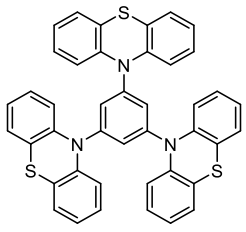 **3PTZ** *Energy Environ. Sci.* **2020**, *13*, 4142-4156.	active material: Super P: PVDF = 4: 4: 2	120	31 (1 C) 9 (20 C) 1 C = 120 mAh g^{-1}	66%/100/1 C	3-4V
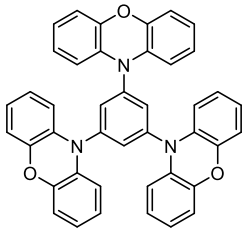 **3PXZ** *Energy Environ. Sci.* **2020**, *13*, 4142-	active material: Super P: PVDF = 4: 4: 2	129	99 (1 C) 76 (20 C) 1 C = 120 mAh g^{-1}	65%/100/1 C	3-4V

4156.					
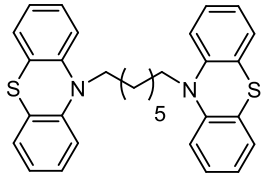 **2PTZ-C_7H_{14}** *Adv. Mater.* **2024**, *36*, 2312486.	active material: Super P: PVDF = 4: 4: 2	104	98 (1 C) 64 (10 C)	60%/1000/1 C	3-4V
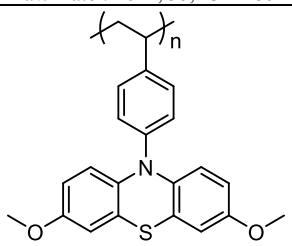 **P-PhPTZOMe** *J. Power Sources* **2024**, *612*, 234779.	active material: Super P: PVDF = 9: 1: 1	148	109 (1 C) 101 (10 C) 94 (20 C) 1 C = 148 mAh g^{-1}	81%/800/1 C	2.8-4.1V
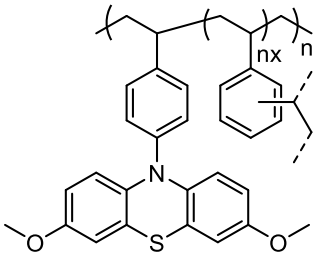 **X-PSDMPT** *ACS Appl. Polym. Mater.* **2024**, 6, 7956-7968.	active material: Super P: PVDF = 6: 3: 1	143	125 (0.5 C) 123 (1 C) 56 (50 C) 10 (100 C) 1 C = 143 mAh g^{-1}	96%/550/1 C	3.1-4.2V

References

[S1] Zhang, S.; Cai, J.; Li, H.; Xing, F.; Chen, L.; Wang, X.; He, X. Two-Electron Phenothiazine Based Cathode Achieved by Raising HOMO Energy Level for High Performance Lithium Organic Battery. *Adv. Energy Mater.* **2025**, *15*, 2403029.

[S2] Frisch, M. J.; Trucks, G. W.; Schlegel, H. B.; Scuseria, G. E.; Robb, M. A.; Cheeseman, J. R.; Scalmani, G.; Barone, V.; Petersson, G. A.; Nakatsuji, H.; Li, X.; Caricato, M.; Marenich, A. V.; Bloino, J.; Janesko, B. G.; Gomperts, R.; Mennucci, B.; Hratchian, H. P.; Ortiz, J. V.; Izmaylov, A. F.; Sonnenberg, J. L.; Williams-Young, D.; Ding, F.; Lipparini, F.; Egidi, F.; Goings, J.; Peng, B.; Petrone, A.; Henderson, T.; Ranasinghe, D.; Zakrzewski, V. G.; Gao, J.; Rega, N.; Zheng, G.; Liang, W.; Hada, M.; Ehara, M.; Toyota, K.; Fukuda, R.; Hasegawa, J.; Ishida, M.; Nakajima, T.; Honda, Y.; Kitao, O.; Nakai, H.; Vreven, T.; Throssell, K.; Montgomery, J. A., Jr.; Peralta, J. E.; Ogliaro, F.; Bearpark, M. J.; Heyd, J. J.; Brothers, E. N.; Kudin, K. N.; Staroverov, V. N.; Keith, T. A.; Kobayashi, R.; Normand, J.; Raghavachari, K.; Rendell, A. P.; Burant, J. C.; Iyengar, S. S.; Tomasi, J.; Cossi, M.; Millam, J. M.; Klene, M.; Adamo, C.; Cammi, R.; Ochterski, J. W.; Martin, R. L.; Morokuma, K.; Farkas, O.; Foresman, J. B.; Fox, D. J., Gaussian, Inc., Wallingford, CT, USA, **2016**.

[S3] Lindström, H.; Södergren, S.; Solbrand, A.; Rensmo, H.; Hjelm, J.; Hagfeldt, A.; Lindquist, S.-E. Li^+ Ion Insertion in TiO_2 (Anatase). 2. Voltammetry on Nanoporous Films. *J. Phys. Chem. B* **1997**, *101*, 7717-7722.

[S4] Liu, T. C.; Pell, W. G.; Conway, B. E.; Roberson, S. L. Behavior of Molybdenum Nitrides as Materials for Electrochemical Capacitors: Comparison with Ruthenium Oxide. *J. Electrochem. Soc.* **1998**, *145*, 1882-1888.

[S5] (a) Luo, L.-W.; Ma, W.; Dong, P.; Huang, X.; Yan, C.; Han, C.; Zheng, P.; Zhang, C.; Jiang, J.-X. Synthetic Control of Electronic Property and Porosity in Anthraquinone-Based Conjugated Polymer Cathodes for High-Rate and Long-Cycle-Life Na–Organic Batteries. *ACS Nano* **2022**, *16*, 14590-14599. (b) Wang, Y.; Bai, P.; Li, B.; Zhao, C.; Chen, Z.; Li, M.; Su, H.; Yang, J.; Xu, Y. Ultralong Cycle Life Organic Cathode Enabled by Ether-Based Electrolytes for Sodium-Ion Batteries. *Adv. Energy Mater.* **2021**, *11*, 2101972. (c) Tao, R.; Zhang, T.; Tan, S.; Jafta, C. J.; Li, C.; Liang, J.; Sun, X.-G.; Wang, T.; Fan, J.; Lu, Z.; Bridges, C. A.; Suo, X.; Do-Thanh, C.-L.; Dai, S. Insight into the Fast-Rechargeability of a Novel Mo1.5W1.5Nb14O44 Anode Material for High-Performance Lithium-Ion Batteries. *Adv. Energy Mater.* **2022**, *12*, 2200519.